JOURNAL OF COMPUTATIONAL PHYSICS 91, 381–397 (1990)

An Improved Pseudospectral Method for Initial-Boundary Value Problems

BENGT FORNBERG

Corporate Research, Exxon Research and Engineering Company, Annandale, New Jersey 08801

Received May 30, 1989; revised November 30, 1989

Pseudospectral methods are commonly used to obtain accurate solutions to initial-boundary value problems. Especially with second (or higher) order derivatives in space, the corresponding differentiation matrices tend to have large spurious eigenvalues (leading, for example, to severe time step restrictions in case of explicit time-stepping methods). We introduce here a new procedure for incorporating boundary conditions, which reduces spurious eigenvalues by an order of magnitude or more (also allowing more freedoms in the choice of grid point locations). © 1990 Academic Press, Inc.

1. INTRODUCTION

Pseudospectral (PS) methods are, in many applications, attractive alternatives to finite difference (FD) methods. Originally, PS methods were most often thought of in terms of expansions in some function space (trigonometric series, orthogonal polynomials, etc., e.g. [1, 5]). Another viewpoint (exclusively taken in this study) is to consider PS methods as special cases of very high order FD methods. For periodic problems, the Fourier–PS method represents the limit of FD methods when the order of accuracy (and width of FD stencils) tends to infinity [2, 4]. In this limit, typical stability conditions for explicit methods remain $\Delta t = O(1/N)$ and $\Delta t = O(1/N^2)$ in cases of first and second derivatives in space. In connection with popular time-stepping methods, such as a fourth-order Runge–Kutta method, the above-eight-order accuracy in space tends to make the time steps limited by accuracy rather than by stability.

In the presence of boundaries, PS methods no longer correspond to FD methods with stencil widths tending to infinity (across periodic repetitions of the data), but rather to FD methods extending over only one set of the grid points. Another fundamental difference is that whatever distribution of grid- (collation-) points is used, at least some weights will diverge as N is increased. In the case of equidistant points, the largest weights (occurring for approximations to derivatives at points near the boundaries) will grow exponentially with N. By clustering the grid points towards the boundaries, for example, as in the Chebyshev method ($x_j = -\cos \pi j/N$, $j = 0, 1, ..., N$, for the interval $[-1, 1]$), the growth rate is reduced to polynomial in

0021-9991/90 $3.00

N. However, "spurious eigenvalues" are introduced (worsening typical explicit time step restrictions to $\Delta t = O(1/N^4)$ in case of second derivatives in space).

The two main ideas which will be pursued in this study are:

1. We introduce a parameter α such that $\alpha = 0$ and $\alpha = 0.5$ correspond to equi-spaced and Chebyshev grids, respectively. All test results are given for the range $0 \leqslant \alpha \leqslant 0.6$ (the fact that only the case $\alpha = 0.5$ corresponds to a well-known class of orthogonal polynomials appears to be of no consequence).

2. The boundary difficulties in PS methods can be traced to the "Runge-phenomenon": violent oscillations of interpolating polynomials near the ends of an interval (the Chebyshev method suppresses these by clustering the grid points there). The following example suggests a complementary strategy: Assume we are to solve

$$u_t = u_{xx} \tag{1}$$

with initial condition

$$u(x, 0) = f(x) \tag{2}$$

and boundary conditions

$$u(\pm 1, t) = 0. \tag{3}$$

The standard PS approach incorporates (3), but ignores its immediate consequences $u''(\pm 1) = 0$, $u^{(4)}(\pm 1) = 0$, etc. Any similar "extra" conditions (obtained from differentiated versions of the equation and the boundary conditions) are in general inconsistent with the Runge oscillations and can be used to suppress them. Suitably incorporated into differentiation matrices, they are found to sharply reduce their largest eigenvalues as well as their norms (both critical quantities in connection with time step restrictions, as clarified in recent studies by L. N. Trefethen *et al.* [9, 10]) without any adverse effects on the accuracy.

The proposed numerical procedure can be seen as a "filter"-method. Since it amounts to a low rank update of a "regular" spectral method, fast transform algorithms (like FFTs in case of the Chebyshev node distribution) can still be utilized. Alternatively, the complete scheme can be implemented by means of (full) matrix × vector multiplications. Although this costs $O(N^2)$ operations per time step vs $O(N \log N)$ for the fastest transform-based case, the multiplication method is still faster on most modern computers unless N is quite large ($\geqslant 100$ according to [8]). In this study, we take the matrix × vector approach because of its flexibility and conceptual simplicity.

In the following sections (2–5), we discuss:

2. Generation of elements of differentiation matrices; typical sizes of their elements;

3. Incorporation of "extra" boundary information;

4. The eigenvalues of the differentiation matrices, their L^2-norms, measures of "normality," etc.

5. Concluding observations and heuristic interpretations.

2. Differentiation Matrices

Given $N+1$ grid points x_j, $-1=x_0\leqslant x_1\leqslant\cdots\leqslant x_N=1$, PS differentiation matrices D^k for derivatives of orders $k=1$ and 2 can be written down in a closed form which is well suited for numerical calculation [7]. Here D^k denotes an $(N-1)\times(N-1)$-matrix in which row j contains the weights in the approximation of d^k/dx^k at $x=x_j$. Alternatively, the algorithm in [3] can be used for any value of k (although this results in a higher operation count when $k=1$ or 2).

With an equi-spaced grid ($x_j=-1+2j/N$, $j=0, 1, \ldots, N$) and second-order accurate finite differences, the standard FD approximation to d^d/dx^2 corresponds to the differentiation matrix

$$\mathrm{D}^2_{\mathrm{FD}}=\begin{bmatrix} -2 & 1 & & & \\ 1 & -2 & 1 & & \\ & \cdot & \cdot & \cdot & \\ & & \cdot & \cdot & \cdot \\ & & & 1 & -2 \end{bmatrix}\times N^2/4. \tag{4}$$

Figure 1a displays graphically the elements of this matrix in the case of $N=10$. With the same vertical scaling, Figs. 1b and c show the corresponding PS matrices on equi-spaced and Chebyshev grids, respectively. The different character of these two PS cases is even more striking when $N=20$ (Figs. 2a and b; note that the

TABLE I

Different Distributions of Grid Points in the Interval $[-1, 1]$

	Node locations x_j, $j=0, 1, \ldots, N$	Local density of nodes (as function of x; $0\leqslant x\leqslant 1$)	Constants c_α s.t. $\int_{-1}^{1} d_\alpha(x)\,dx=1$
Equi-spaced	$x_j=-1+2j/N$	$d_0(x)=\frac{1}{2}\left(=\frac{c_0}{(1-x^2)^0}\right)$	$c_0=\frac{1}{2}$
Chebyshev	$x_j=-\cos(\pi j/N)$	$d_{1/2}(x)=\frac{c_{1/2}}{(1-x^2)^{1/2}}$	$c_{1/2}=\frac{1}{\pi}$
Generalized distribution ($\alpha<1$)	$\frac{j}{N}=\int_{-1}^{x_j} d_\alpha(t)\,dt$	$d_\alpha(x)=\frac{c_\alpha}{(1-x^2)^\alpha}$	$c_\alpha=\frac{\Gamma(3/2-\alpha)}{\pi^{1/2}\Gamma(1-\alpha)}$

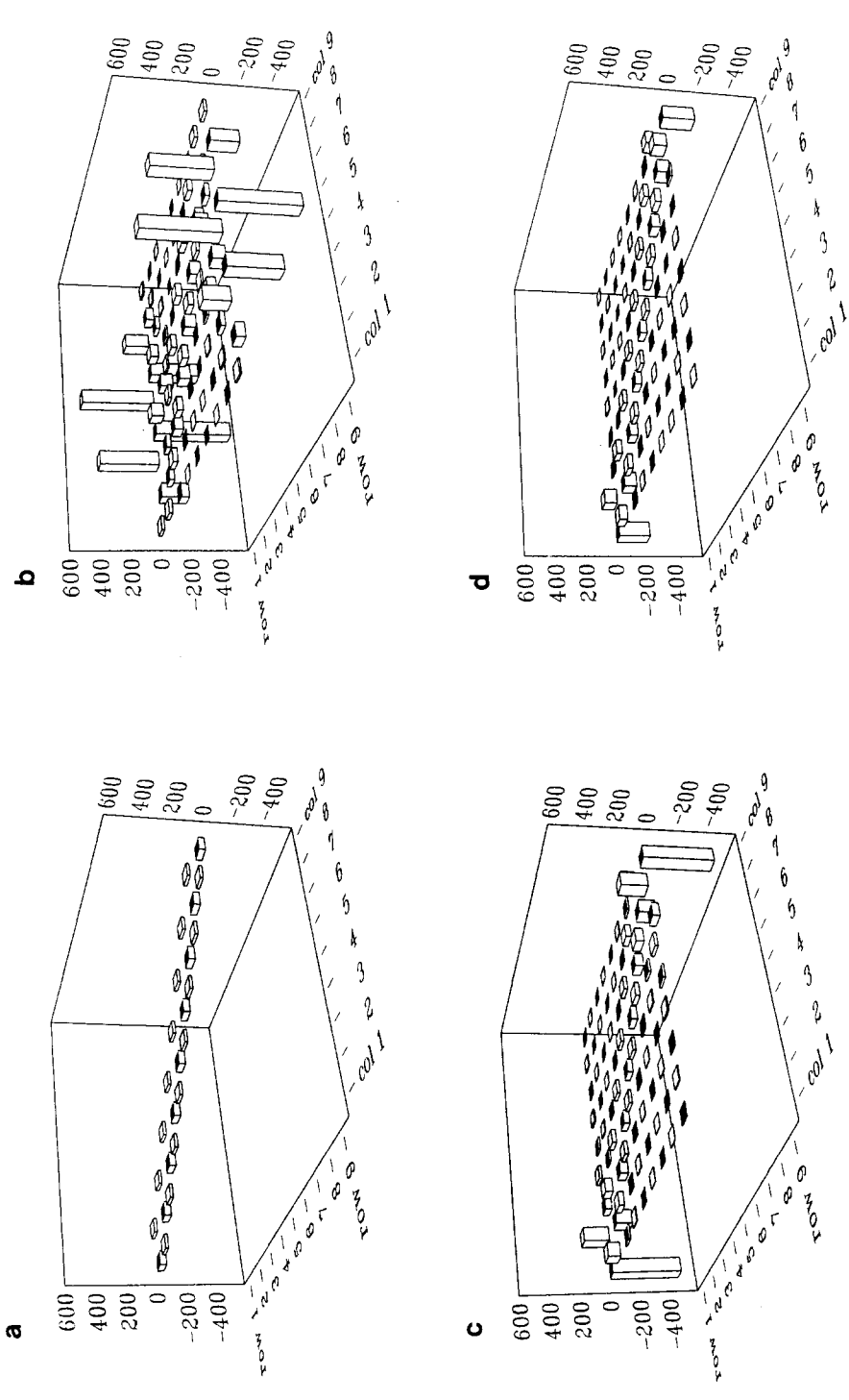

FIG. 1. Examples of differentiation matrices, $N = 10$: (a) Second-order FD; (b) PS method, equi-spaced grid; (c) PS method, Chebyshev grid; (d) PS method, $\alpha = 0.4$.

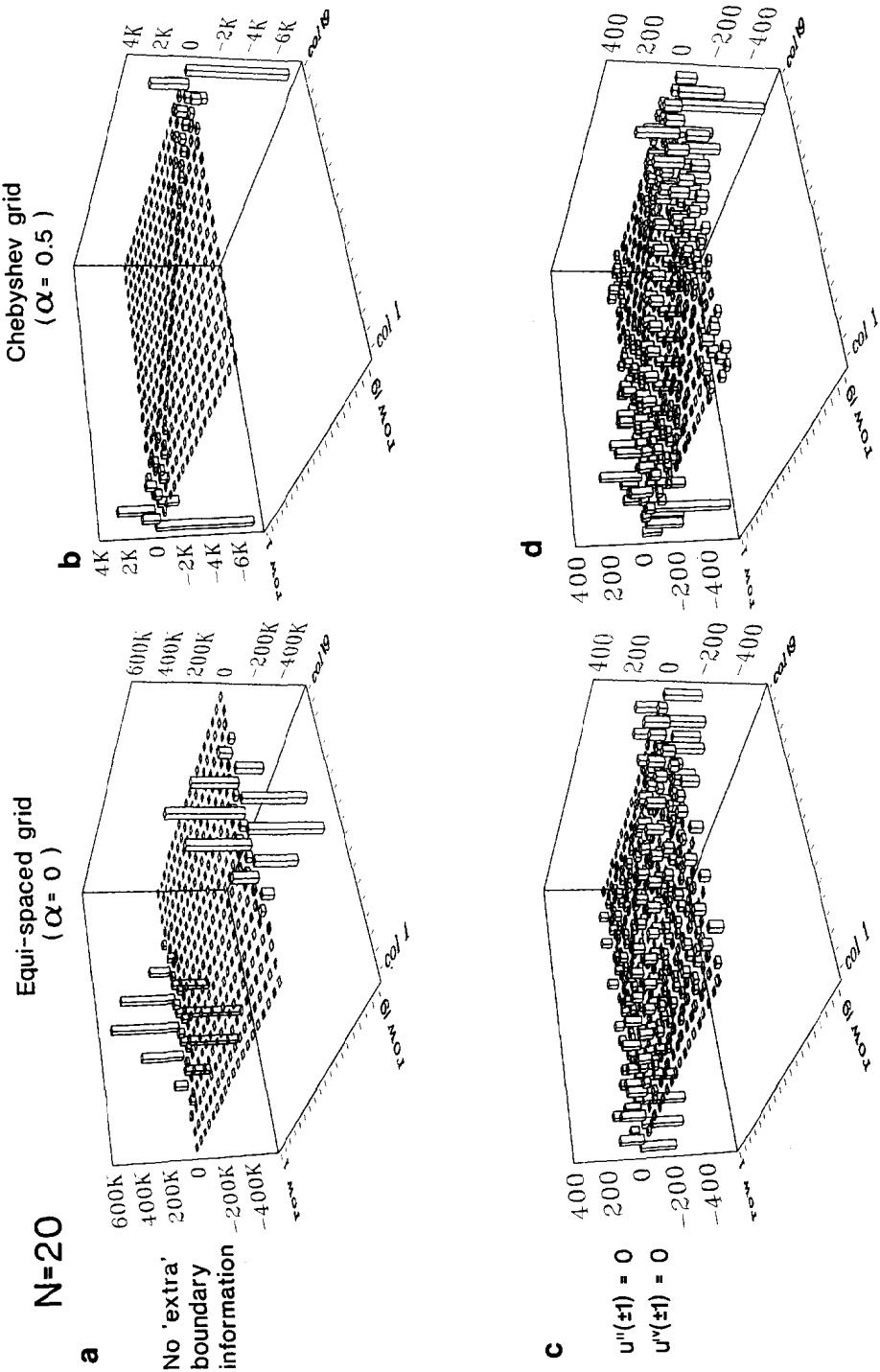

FIG. 2. Examples of PS differentiation matrices, $N = 20$.

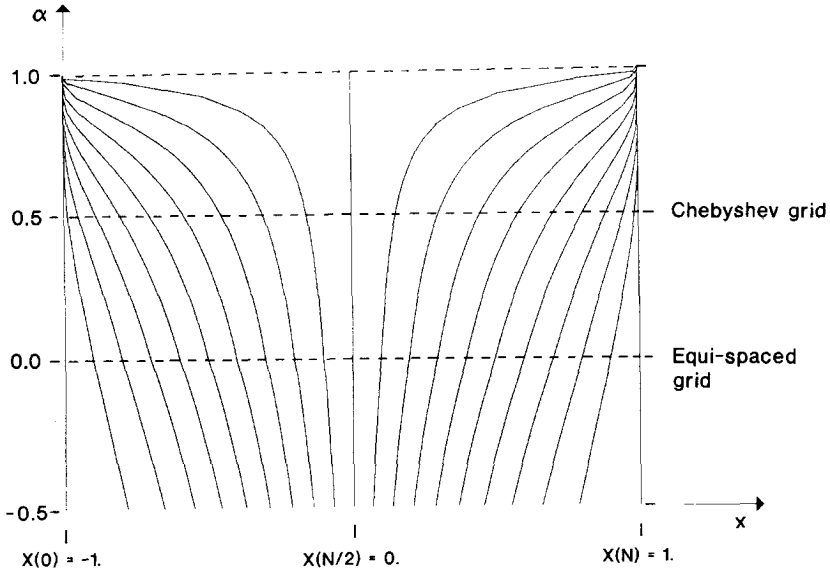

FIG. 3. The distribution of grid points for α between -0.5 and $+1.0$ (displayed for $N=20$).

vertical scales here differ by a factor of 100). The largest elements grow like $O(2^N N^{-1/2} \log N)$ and $O(N^4)$, respectively.

It is natural to ask whether "intermediate" node distributions could prove advantageous. Noting the relations shown in Table I, we introduce such grids by means of

$$\frac{j}{N} = \frac{\Gamma(3/2-\alpha)}{\pi^{1/2}\Gamma(1-\alpha)} \int_{-1}^{x_j} \frac{dt}{(1-t^2)^\alpha}, \qquad j=0, 1, ..., N, \alpha < 1. \tag{5}$$

Figure 3 illustrates how these grid points move with α. Figure 1d shows the differentiation matrix for $\alpha = 0.4$ (suggesting a slight reduction in norm as well as a small improvement in symmetry). However, as we will see in Sections 3 and 4 (and as was noted in [7], where a different continuation between equi-spaced and Chebyshev grids was considered), variation of α alone will not improve either accuracy or stability (apart from for very low values of N).

3. Incorporation of Additional Boundary Information

As Figs. 1b and 2a indicated (in the "extreme" case of $\alpha = 0$), weights for the approximations to d^2/dx^2, at the first few interior gridpoints, are highly oscillatory (and are largest near the center of the grid). The same is true for approximations

to any derivative at the boundary itself (not part of the differentiation matrix). If we again consider the model problem (1)–(3) or the eigenvalue problem

$$\begin{aligned} u_{xx} &= \lambda u \\ u(\pm 1) &= 0 \end{aligned} \tag{6}$$

we know that d^k/dx^k is zero at both boundaries for $k = 0, 2, 4, \ldots$, etc. We can add/subtract multiples of the corresponding difference formulas from each row of the differentiation matrix, for example, to minimize the L^2-norm of each row. The bottom two diagrams in Fig. 2 (c and d) show the effect of using two "extra" conditions at each boundary. Reductions in element sizes of orders 1000 and 10 are seen for $\alpha = 0$ and $\alpha = 0.5$, respectively. The resulting matrices look relatively similar in the two cases.

4. Eigenvalues of Differentiation Matrices

Equation (6) has eigenvalues

$$\lambda_k = -\left(\frac{k\pi}{2}\right)^2, \qquad k = 1, 2, 3, \ldots \tag{7}$$

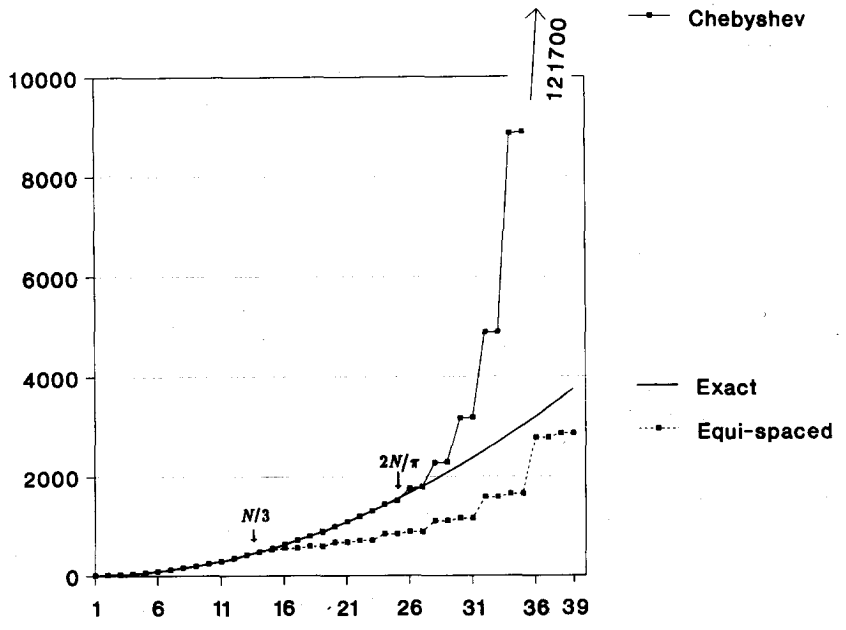

FIG. 4. Magnitudes of eigenvalues of PS differentiation matrices (equi-spaced and Chebyshev grids) compared to analytic eigenvalues, $N = 40$.

with corresponding eigenfunctions

$$u(x) = \begin{cases} \cos(\frac{1}{2}k\pi x) & , k \text{ odd}, \\ \sin(\frac{1}{2}k\pi x) & , k \text{ even}. \end{cases} \tag{8}$$

Weideman and Trefethen [11] studied the eigenvalues of PS differentiation matrices for solving (6). They noted that these followed the pattern shown in Fig. 4 (displayed here for $N = 40$). They also showed that the largest eigenvalue grows at a rate of $0.048 \times N^4$ (a lower rate than for grids based on Legendre or Chebyshev zeros, which lead to $0.102 \times N^4$ and $0.303 \times N^4$, respectively).

The left columns of diagrams in Figs. 5 and 6 ($N = 16$ and $N = 64$, respectively) show how the computed eigenvalues vary with α and with the number of "extra" items of boundary information that have been incorporated. Eigenvalues in magnitude exceeding 2000 and 35,000, respectively, have been reduced to these values, with the true values for the largest ones indicated explicitly for $\alpha = 0.5$ and $\alpha = 0.6$. The right columns show $\log_{10}$ of the magnitude of the errors in the eigenvalues (compared to their analytical values (7); the surfaces have not been drawn below the level -10, i.e., errors $< 10^{-10}$).

With no "extra" boundary information (top row in the Figs. 5 and 6), values of α above 0.5 are seen to be unacceptable both because of lost accuracy and because of extreme growth of large spurious eigenvalues. Values of α less than 0.5 also lead to lost accuracy (for large N) and (not visible in these figures) to a near-catastrophic growth in the norm of the differentiation matrix. With "extra" boundary information incorporated, a range of α's $\leqslant 0.5$ opens up throughout which the accuracy remains consistently high.

A close look at the diagrams a – d in Figs. 5 and 6 show that, for every "extra" boundary condition used (at either end), the largest remaining spurious eigenvalue has been reduced to exactly zero. This is a consequence of the least squares processes; each modified differentiation matrix has a null-space spanned by the vectors representing the "extra" boundary conditions. As the "extra" boundary information is consistent with the physically relevant eigenmodes, they have remained largely unaffected.

Figures 7a–c show how the α-interval, featuring the highest accuracies, varies with N (shown for $N = 8$, 32, and 128, respectively, in order to complement the data in Figs. 5 and 6; each curve corresponds to a cross section in these figures, placed at the eigenvalue number $N/2 - 1$). In this and the following figures, the labels for the curves (0–3) identify how many "extra" items of information were applied at each boundary. The regular Chebyshev case (0 "extra" boundary conditions, $\alpha = 0.5$) is marked by a solid black dot.

Figures 8a–c show the magnitudes of the largest eigenvalues. They are seen to be much reduced throughout the α-range which corresponds to the best accuracy (and they go down significantly with each "extra" boundary condition that is applied).

Figures 9a–c show similarly the L^2-norms of the differentiation matrices. Again, the values are seen to be strongly reduced for each "extra" boundary condition, and

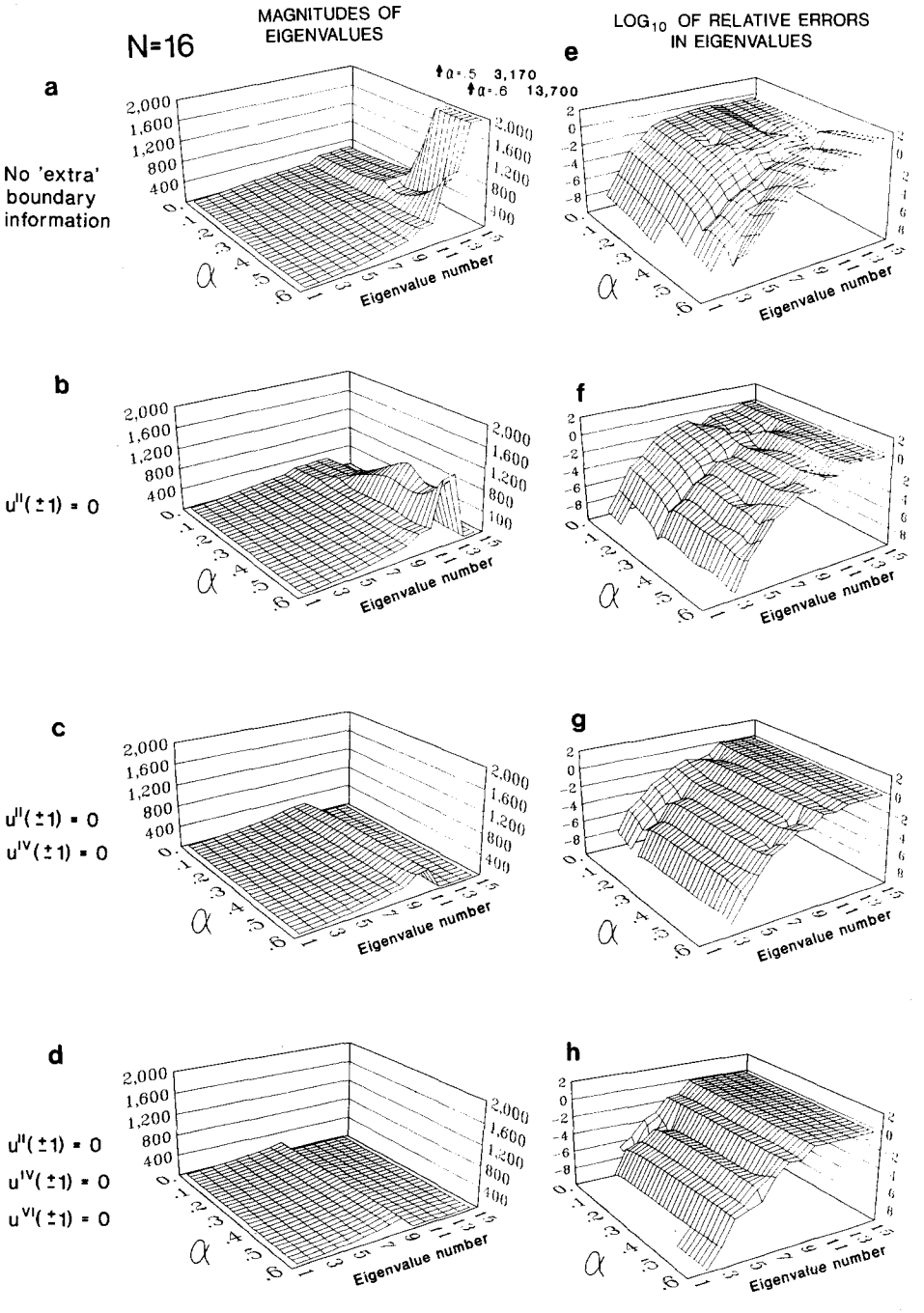

FIG. 5. Magnitude of eigenvalues and $\log_{10}$ of their relative errors, $N = 16$.

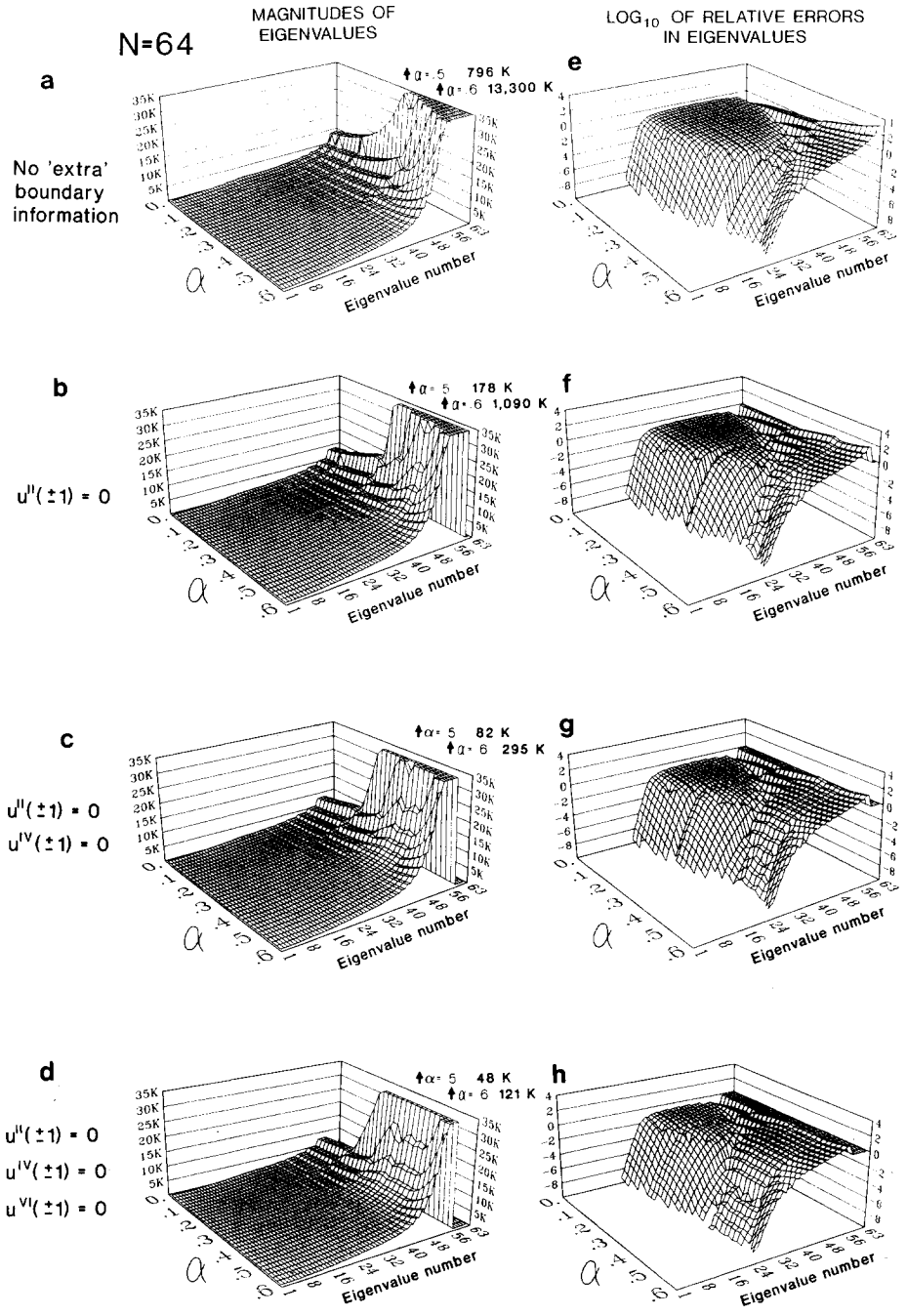

FIG. 6. Magnitude of eigenvalues and $\log_{10}$ of their relative errors, $N = 64$.

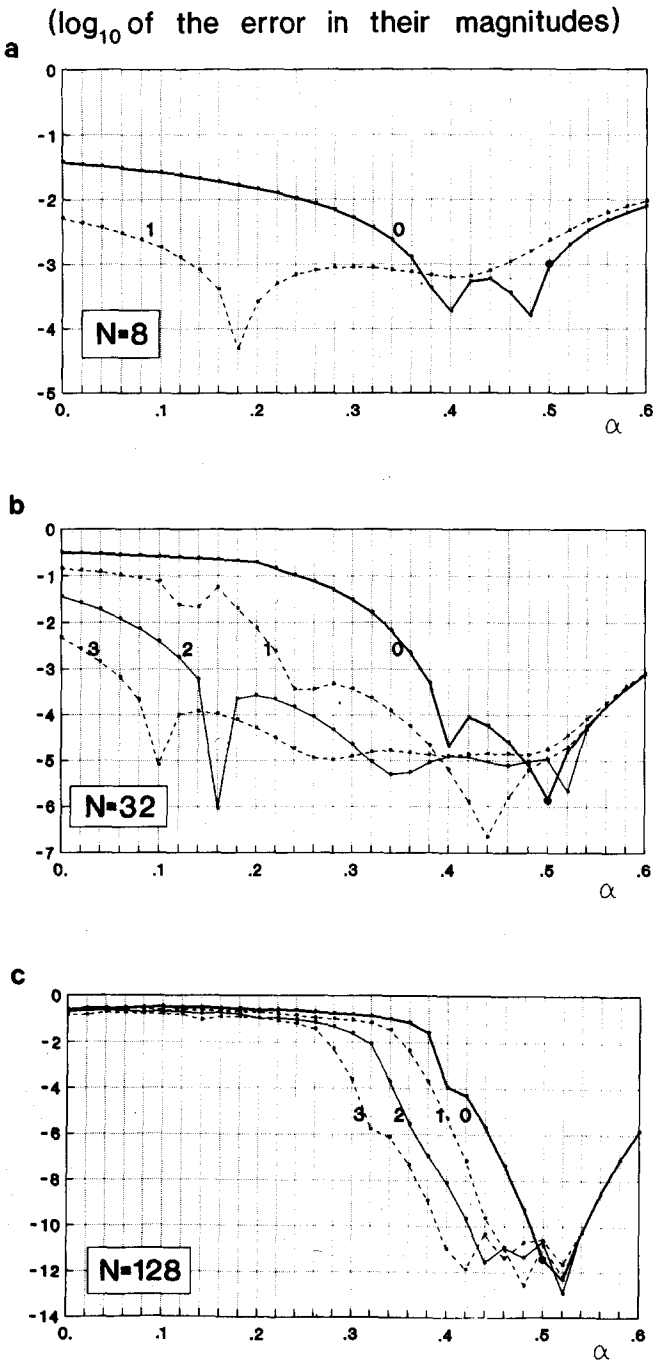

FIG. 7. Accuracies of the $(N/2-1)$th eigenvalue for different α and $N=8$, 32, and 128.

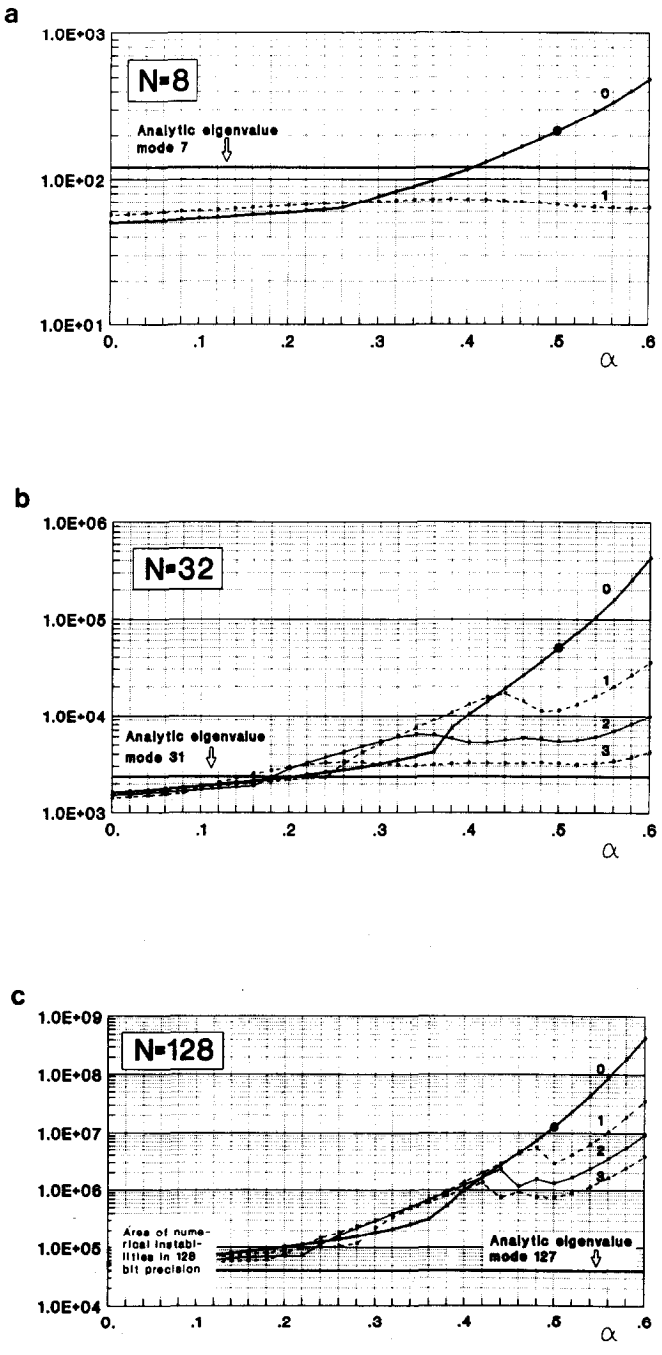

FIG. 8. Largest eigenvalue (in magnitude) for different α and $N = 8$, 32, and 128.

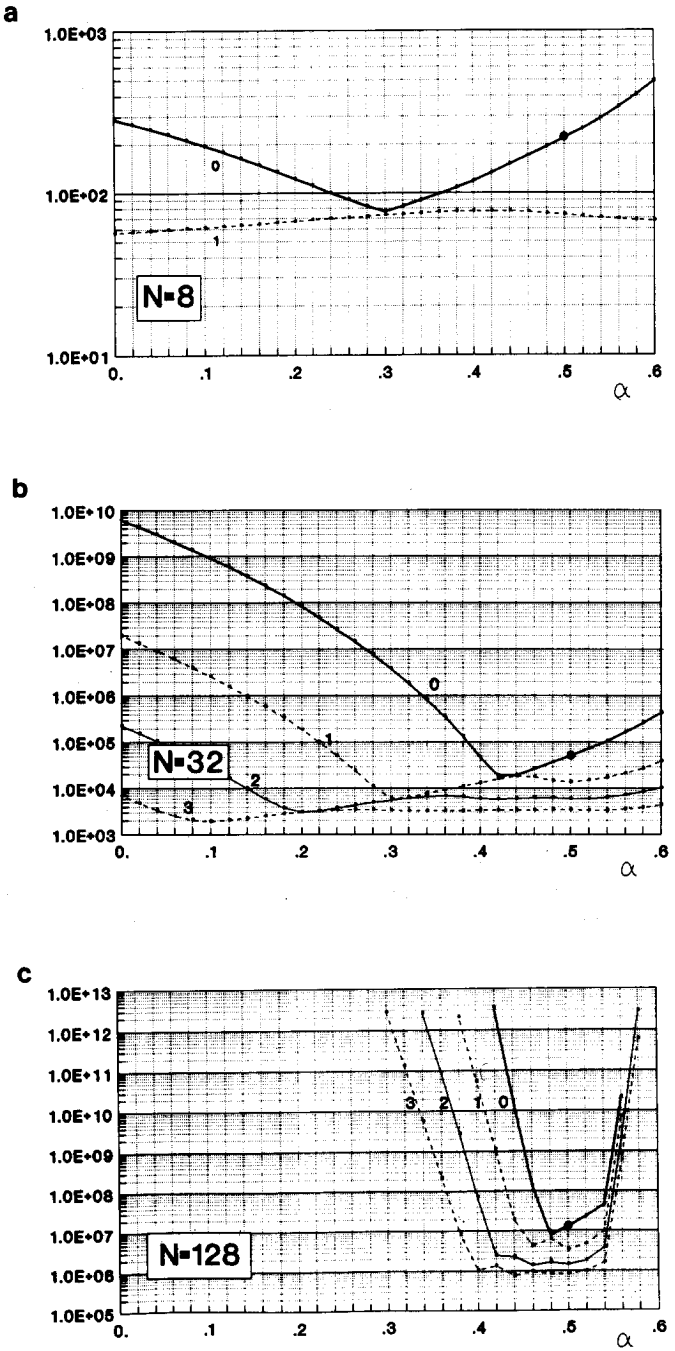

FIG. 9. L^2-norms for different α and $N = 8$, 32, and 128.

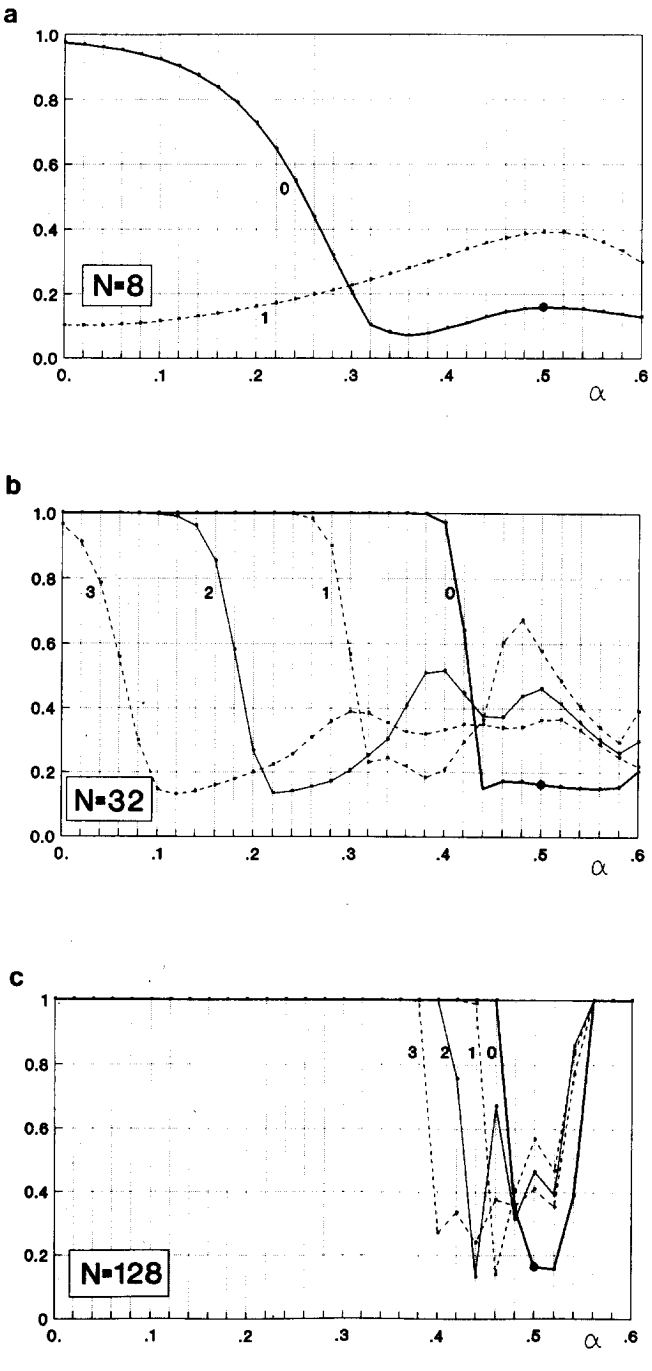

FIG. 10. Size of commutator for different α and $N = 8$, 32, and 128.

they keep a comparatively constant level across the α-range which featured the highest accuracy.

The matching reductions in both largest eigenvalue and L^2-norm imply corresponding improvements in "eigenvalue stability" and "Lax stability" [10] or similarly "time-" and "space-" stabilities [6, 7], i.e., the limits of $t \to \infty$, N fixed, and $N \to \infty$, t fixed, respectively.

Figures 10a–c show still another measure of the differentiation matrices, the size of their "commutators":

$$C(D) = \frac{\|D^T D - DD^T\|_2}{\|D^T D\|_2}. \tag{9}$$

This quantity always satisfies $0 \leqslant C(D) \leqslant 1$ and is equal to zero if and only if D is "normal," i.e., has a full set of orthogonal eigenvectors. The "normality" is seen to be good throughout the α-ranges of interest.

5. Concluding Observations

The technique of modifying the differentiation matrices by "extra" items of boundary information (derived from the original equations) has been found to

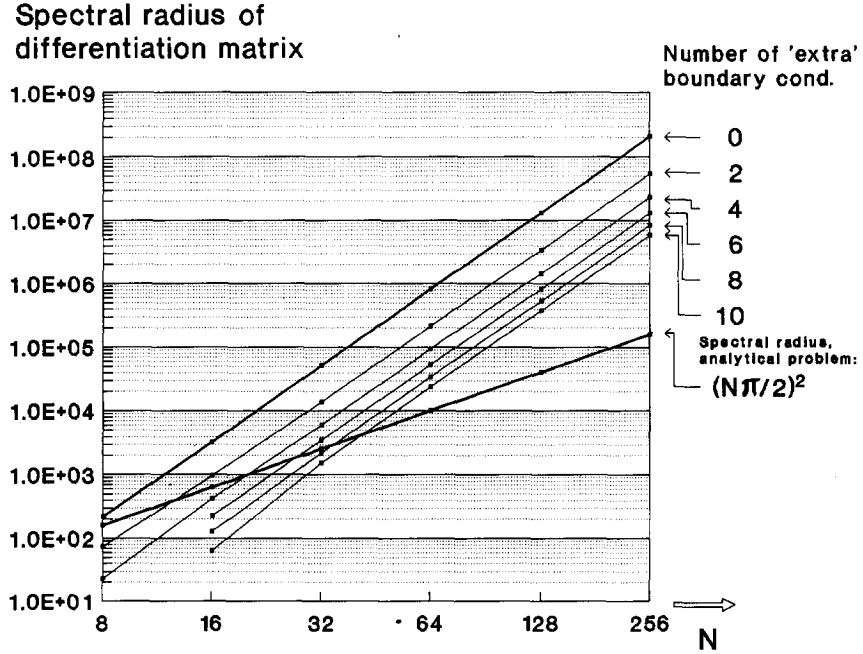

FIG. 11. Spectral radius of differentiation matrix for different numbers of "extra" boundary conditions ($\alpha = 0.5$).

significantly reduce both the norms and the largest spurious eigenvalues of spectral differentiation matrices. Without this technique, grids need to feature a quadratic (type $\alpha = 0.5$)-clustering of points near the ends. With it, considerably greater freedom is obtained (without any loss in accuracy). There is no need for a grid to feature the same type of clustering (or for the same number of "extra" boundary conditions to be used) at both boundaries.

It is trivial to differentiate the model equation (1) any number of times (and thus, to generate any number of "extra" boundary conditions). In most equations of practical interest (involving variable coefficients, nonlinearities, more involved primary boundary conditions, more space dimensions, etc.), the algebraic complexity is likely to be more severe. Therefore, this study has focused on the use of only a few "extra" boundary conditions. Mainly for theoretical interest, Figs. 11 and 12 are included to show the trends if large numbers of "extra" boundary conditions can be used. Figure 11 shows that the reduction in spectral radius (for each "extra" boundary condition) is essentially independent of N.

The number of "extra" boundary conditions might alternatively be chosen as a fixed fraction of N. Since there only are about $(1 - 2/\pi) \times N \approx 0.35N$ spurious eigenvalues (in the case $\alpha = 0.5$; cf. Fig. 4), it is most natural to focus on fractions smaller than 0.35. The results in Fig. 12 suggest that the growth rates in these cases get

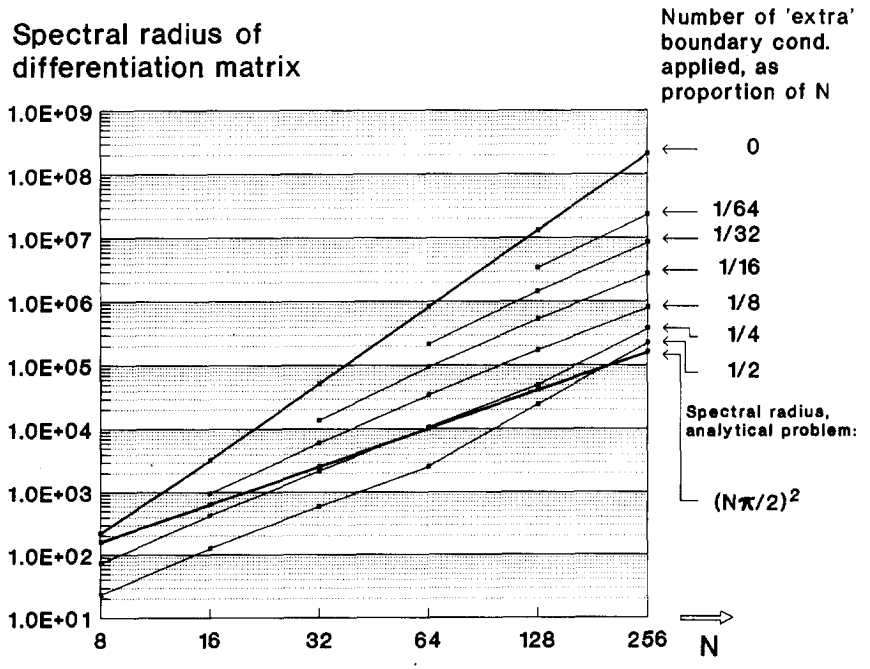

FIG. 12. Spectral radius of differentiation matrix for different ratios of numbers of "extra" boundary conditions to N ($\alpha = 0.5$).

sharply reduced, from $O(N^4)$ to something well below $O(N^3)$ (possibly as low as $O(N^2)$ for N sufficiently large).

Returning to the right column of diagrams in Fig. 6, the "valley" at $\alpha = 0.5$ in Fig. 6e reflects the well-known high accuracy of Chebyshev approximations. Its minimax error for interpolation is within a small factor $(4 + (2/\pi)\log N)$ of the lowest possible limit for any polynomial. Heuristically, it seems likely that it is this limit for the optimal polynomial which prevents further gains in absolute accuracy in the near-constant high accuracy region extending down from $\alpha = 0.5$ in Figs. 6f, g, and h. At $\alpha = 0.5$ a "crossover" occurs as the accuracy (for $\alpha > 0.5$) instead becomes limited by the depletion of points near the center of the domain (no longer allowing $2/\pi$ of the modes present to be resolved). The third "barrier," limiting accuracy for low values of α (i.e., preventing the use of near-equi-spaced grids), has been the topic of this study. The method of "extra" boundary information has allowed us to shift this barrier down towards lower values of α.

REFERENCES

1. C. CANUTO, M. Y. HUSSANI, A. QUARTERONI, AND T. ZANG, *Spectral Methods in Fluid Dynamics* (Springer Verlag, New York, 1988).
2. B. FORNBERG, *Geophysics* **52**, 483 (1987).
3. B. FORNBERG, *Math. Comput.* **51**, 699 (1988).
4. B. FORNBERG, *SIAM J. Numer. Anal.* **27**, 904 (1990).
5. D. GOTTLIEB AND S. A. ORSZAG, *Numerical Analysis of Spectral Methods: Theory and Applications* (SIAM, Philadelphia, 1977).
6. D. GOTTLIEB, S. A. ORSZAG, AND E. TURKEL, *Math. Comput.* **37**, 293 (1980).
7. A. SOLOMONOFF AND E. TURKEL, *J. Comput. Phys.* **81**, 239 (1989).
8. T. D. TAYLOR, R. S. HIRSH, AND M. M. NADWORNY, *Comput. Fluids* **12**, 1 (1984).
9. L. N. TREFETHEN AND M. R. TRUMMER, *SIAM J. Num. Anal.* **24**, 1008 (1987).
10. L. N. TREFETHEN, in *Numerical Methods for Fluid Dynamics III*, edited by K. W. Morton and M. J. Baines (Clarendon Press, Oxford, 1988), p. 237.
11. J. A. C. WEIDEMAN AND L. N. TREFETHEN, *SIAM J. Num. Anal.* **25**, 1279 (1988).